[4]Reference 1, Sec. III D.
[5]F. Rosenberger and F. Lüty, Solid State Commun. **7**, 983 (1969).
[6]H. Ohkura, T. Fujiwara, and Y. Mori, J. Phys. Soc. Jap. **29**, 799 (1970).
[7]Reference 1, Sec. III A.
[8]D. Smith (unpublished), reported in Ref. 1, pp. 192–193.
[9]W. Weber and B. G. Dick, Phys. Status Solidi **36**, 723 (196
[10](a) R. C. Alig, Phys. Rev. B 2, 2108 (1970); (b) K. Kojima, N. Nishimaki, and T. Kojima, J. Phys. Soc. Jap. **16**, 2033 (1961); R. A. Evarestov, Phys. Status Solidi **35**, K157 (1969).
[11]For a review of theoretical approaches and results, see W. B Fowler, in Ref. 1, Chap. 2, Sec. III A.1.
[12]R. H. Bartram, A. M. Stoneham, and P. Gash, Phys. Rev. **176**, 1014 (1968).
[13]B. S. Gourary and F. J. Adrian, Phys. Rev. **105**, 1180 (1957).
[14]R. J. Brown and J. M. Vail, Phys. Status Solidi **40**, 737 (1970).
[15]R. J. Brown and J. M. Vail, Phys. Status Solidi B **49**, K33 (1972).
[16]Reference 1, Sec. IV C.
[17]M. Born and K. Huang, *Dynamical Theory of Crystal Lattice* (Oxford U. P., Oxford, England, 1954), Table 9, p. 26.
[18]M. P. Tosi, J. Res. Natl. Bur. Stand. (U.S.) **287**, 2 (1967), Table 2.
[19]M. P. Tosi, in *Solid State Physics*, edited by F. Seitz and D Turnbull (Academic, New York, 1964), Vol. 16, Table VIII, column 2, p. 48.
[20]E. W. Kellermann, Philos. Trans. R. Soc. Lond. **238**, 513 (1940).
[21](a) A. M. Stoneham (private communication), see Ref. 21(b), footnote 12; (b) A. M. Stoneham and R. H. Bartram, Phys. Rev. B **2**, 3403 (1970).
[22]J. A. D. Matthew and B. Green, J. Phys. C **4**, L101 (1971).
[23]R. C. Kern, P. Gash, R. H. Bartram, and A. M. Stoneham Bull. Am. Phys. Soc. **16**, 440 (1971), abstract HF6.
[24]H. Kanzaki, J. Phys. Chem. Solids 2, 24 (1957).
[25]J. R. Hardy, J. Phys. Chem. Solids **15**, 39 (1960).
[26]J. M. Vail, Phys. Status Solidi B **44**, 443 (1971).
[27]W. B. Fowler, in Ref. 11, Sec. III B.
[28]L. D. Bogan and D. B. Fitchen, Phys. Rev. B **1**, 4122 (1970).
[29]F. S. Ham, Phys. Rev. Lett. **28**, 1048 (1972).
[30]N. F. Mott and M. J. Littleton, Trans. Faraday Soc. **34**, 485 (1938).
[31]Reference 1, p. 231, and p. 232 item (c).
[32]B. G. Dick and A. W. Overhauser, Phys. Rev. **112**, 90 (1958).
[33]For a current review of the shell model see W. Cochran, Crit. Rev. Solid State Sci. **2**, 1 (1971).
[34]J. R. Hardy, Philos. Mag. **7**, 315 (1962).
[35]P. D. Schulze and J. R. Hardy, Phys. Rev. B **5**, 3270 (1972); Phys. Rev. B **6**, 1580 (1972).
[36]J. M. Vail, Phys. Rev. B 7, 5359 (1973).
[37]R. J. Brown, Ph.D. thesis (University of Manitoba, 1970) (unpublished).

PHYSICAL REVIEW B VOLUME 8, NUMBER 4 15 AUGUST 1973

Phonons in Cinnabar

M. A. Nusimovici and G. Gorre

Department de Physique Cristalline et Chimie Structurale,
Equipe de recherche associée au Centre National de la Recherche Scientifique, n° 15,
Universite de Rennes, Rennes, France
(Received 5 February 1973)

A mixed-valence–Coulomb-force field has been constructed and used to calculate the phonon frequencies for waves propagating in symmetry directions of α-HgS—cinnabar. The model is similar to the one previously used to describe the lattice dynamics of partially ionic semiconducting compounds with wurtzite and zinc-blende structures. The calculated frequencies and velocities of sound are in agreement with the experimental values.

I. INTRODUCTION

There are two polymorphs of mercury sulphide: α-HgS or cinnabar is red and has a trigonal structure (D_3^4); β-HgS or metacinnabar is black and has a cubic structure (T_d^2). The transition takes place at 344 °C under atmospheric pressure.

Cinnabar appears to be a material of considerable interest, since it is a II-VI semiconducting compound with a highly anisotropic structure. It is strongly piezoelectric and it is the most optically active of all known mineral compounds. The promising acousto-optical properties of cinnabar have been recently pointed out by Sapriel.[1] Crystal growth of cinnabar is very difficult. It is only recently that a detailed experimental study of phonon frequencies by Raman scattering[2] was made possible because monocrystals of fairly good quality and size were grown at the Centre National d'Etudes des Telecommunications (Lannion, France).[3]

A fairly extensive study of the long-wavelength vibrations and polaritons in cinnabar has been done by Zallen, Lucovsky, Taylor, Pinczuk, and Burstein.[4]

In this paper, we present the results of a calculation of phonon frequencies in α-HgS–cinnabar. The model is based upon the mixed-valence Coulomb-force-field model previously used to cal-

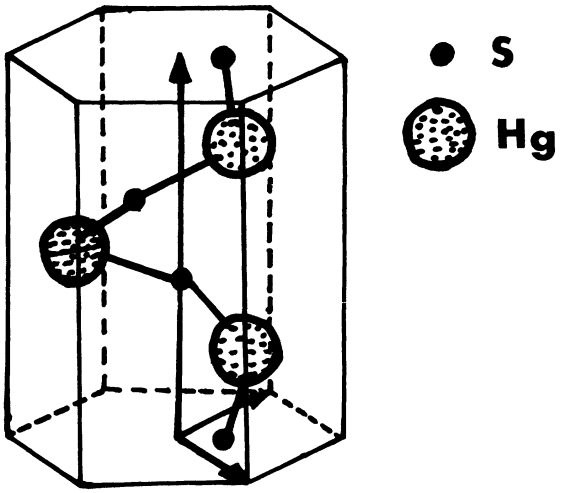

FIG. 1. Elementary cell of cinnabar. The six atoms of the elementary cell belong to the same helix.

culate phonon dispersion in CdS.[5,6] As will be discussed below, the model which we used included short-range forces designed to simulate the covalent-bond contributions and long-range forces whose origin is in the partially ionic nature of the bonding. The six atoms of the elementary cell are placed along an helicoidal chain; one long-range parameter and six short-range parameters were necessary to take into account the main interchain and intrachain interactions. We are not aware of any previous treatment of the lattice dynamics of cinnabar over the whole first Brillouin zone of the reciprocal space. The calculation and the diagonalization of the dynamical matrix is difficult, since the six atoms (3 HgS) of the elementary cell are at sites with much lower symmetry (C_2) than the crystal space group (D_3^4). In order to diagonalize the dynamical matrix in the center of the reciprocal space and to fit the model parameters on experimental frequencies, we had to use group-theoretical considerations based on a detailed study of the crystal space group.

Our calculations are in fairly good agreement with experimental data: infrared[4,7-9] and Raman[2,4-7] spectra and velocities of sound in cinnabar for polarized elastic waves.[1]

TABLE I. Coordinates of the sites of the atoms of the elementary cell ($X=0.72$, $Y=0.48$).

	i	j	k
Hg 1	$\frac{1}{2}aX\sqrt{3}$	$-\frac{1}{2}aX$	$\frac{1}{3}c$
Hg 2	0	aX	$\frac{2}{3}c$
Hg 3	$-\frac{1}{2}aX\sqrt{3}$	$-\frac{1}{2}aX$	0
S 1	$\frac{1}{2}aY\sqrt{3}$	$-\frac{1}{2}aY$	$\frac{5}{6}c$
S 2	0	aY	$\frac{1}{6}c$
S 3	$-\frac{1}{2}aY\sqrt{3}$	$-\frac{1}{2}aY$	$\frac{1}{2}c$

II. SYMMETRY PROPERTIES OF CINNABAR

The structure of cinnabar has been described by Zallen *et al.*[4] The Bravais lattice is based upon the vectors

$$\vec{t}_1=\tfrac{1}{2}a(\sqrt{3})\,\vec{i}-\tfrac{1}{2}a\,\vec{j}\,,\quad \vec{t}_2=a\vec{j}\,,\quad \vec{t}_3=c\vec{k}\,. \qquad (2.1)$$

In Eqs. (2.1), $\vec{i}$, $\vec{j}$, and $\vec{k}$ are the unit vectors of an orthogonal triplet, and c and a are the crystal parameters; their values are, respectively,

$$c=9.497\ \text{Å},\quad a=4.166\ \text{Å}\,.$$

The elementary cell of HgS is shown in Fig. 1; it is made of six ions, the coordinates of which are given in Table I. The nearest, second, and third neighbors of each ion are shown in Fig. 2 and listed in Table II. The symmetry operations of the point group D_3 are shown in Fig. 3 and listed in Table III. The structure consists of helical chains, six atoms to a turn.[10] The nearest neighbors of an ion belong to the same chain as it does, but the second and third neighbors belong to four other chains. Therefore the forces between nearest neighbors are intrachain forces and the forces between second and third neighbors are interchain forces.

The hexagonal first Brillouin zone of cinnabar is shown in Fig. 4. The allowed irreducible representations of the space group at symmetry points of the reciprocal space have been calculated. They

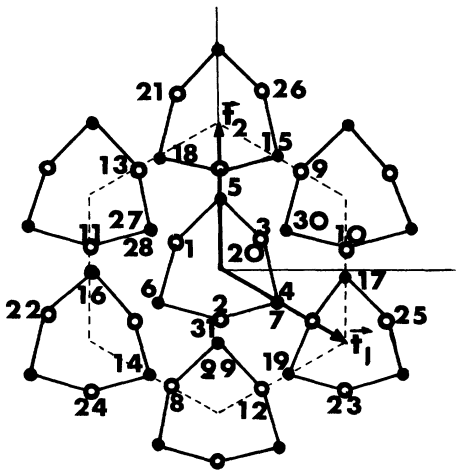

FIG. 2. Nearest, second, and third neighbors of each atom of the elementary cell. The nearest neighbor of an atom belongs to the same chain as it does, but the second and third neighbors belong to four other chains.

TABLE II. Neighbors of each ion in the elementary cell.

		First neighbors		Second neighbors		Third neighbors	
Hg	1	5	6	16	18	29	30
Hg_2	2	6	4	14	19	27	30
Hg_3	3	5	7	15	17	28	29
S_1	4	2	20	10	12	23	25
S_2	5	1	3	9	13	21	26
S_3	6	1	2	8	11	22	24

Length of bonds

First neighbors	Second neighbors	Third neighbors
2.34 Å	3.10 Å	3.31 Å

Angles between first-neighbor bonds

S-Hg-S	172°
Hg-S-Hg	105°

Z coordinate of ions in Fig. 2

0	3	13	26		
$c/6$	5	16	17	29	
$c/3$	1	9	8	21	22
$c/2$	6	18	19	30	
$2c/3$	2	10	11	23	24
$5c/6$	4	14	27		
c	20	12	25		
$-c/6$	7	15	28		
$-c/3$	31				

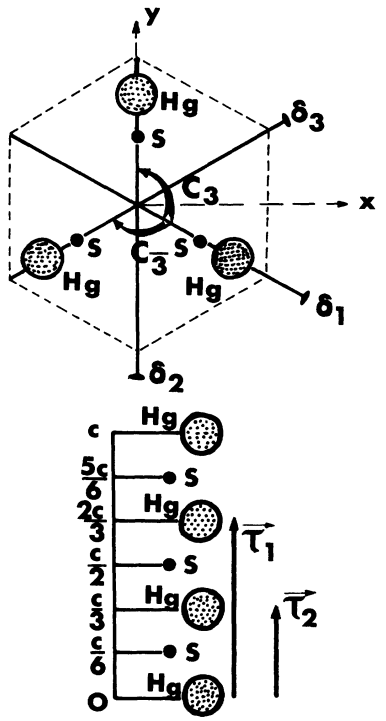

FIG. 3. Symmetry operations of cinnabar (space group D_3^4).

are listed in Table IV. The compatibility relations are given in Table V. Those presentations and compatibility relations have been used to label the computed dispersion curves and to check the symmetries of the normal modes of vibration of the lattice.

III. THEORY

The equations of motion of the ions can be written, in the harmonic approximation, as

$$\omega^2 M_K \vec{u}_\alpha(l,K) = \sum_{l'K'\beta} \phi_{\alpha\beta}\begin{pmatrix} l & l' \\ K & K' \end{pmatrix} \vec{u}_\beta(l',K') \,. \quad (3.1)$$

In Eq. (3.1), $2\pi\omega$ is the frequency of a normal mode, and M_K the mass of the Kth ion of the elementary cell; $u_\alpha(l,K)$ is the αth component of the ionic displacement. The force constants are defined by

$$\phi_{\alpha\beta}\begin{pmatrix} l & l' \\ K & K' \end{pmatrix} = \frac{\partial^2\phi}{\partial u_\alpha(l,K)\partial u_\beta(l'K')} \,. \quad (3.2)$$

The normal coordinates are defined as

$$\vec{w}_\alpha(\vec{k},K) = (M_K/N)^{1/2} \sum_l \vec{u}_\alpha(l,K) e^{-2\pi i \vec{k}\cdot\vec{R}(l,K)} \,. \quad (3.3)$$

In Eq. (3.3), $\vec{R}(l,K)$ is the equilibrium position of

TABLE III. Point group of cinnabar. $\vec{\tau}_1 = \frac{1}{3}c\vec{k}$. $\vec{\tau}_2 = \frac{2}{3}c\vec{k} = 2\vec{\tau}_1$. C_3 and C_3^2 are threefold rotations around the z axis. δ_1, δ_2, and δ_3 are binary rotations around the axis perpendicular to the threefold axis.

Class	Element	Operation
C_1	1	$\{\epsilon \mid \vec{t}\}$
C_2	2	$\{\epsilon \mid \vec{t}\}\{C_3 \mid \vec{\tau}_1\}$
	3	$\{\epsilon \mid \vec{t}\}\{C_3^2 \mid \vec{\tau}_2\}$
C_3	4	$\{\epsilon \mid \vec{t}\}\{\delta_1 \mid \vec{\tau}_2\}$
	5	$\{\epsilon \mid \vec{t}\}\{\delta_2 \mid \vec{\tau}_1\}$
	6	$\{\epsilon \mid \vec{t}\}\{\delta_3 \mid 0\}$

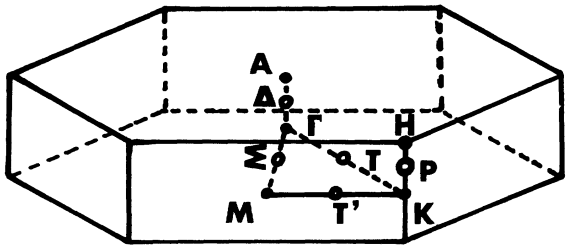

FIG. 4. First Brillouin zone of the reciprocal space of cinnabar.

TABLE IV. Allowed representations of the groups $G_{\vec{k}}/T_{\vec{k}}$ for symmetry vectors $\vec{k}$ of the first Brillouin zone.

Γ	E	C_3	δ	A	E	E'	C_3 C_3^2	C_3^2 C_3	δ_1 δ_2 δ_3	δ_1' δ_2' δ_3'
Γ_1	1	1	1	A_1	$H_1 1$	−1	−1	1	1	−1
Γ_2	1	1	−1	A_2	$H_2 1$	−1	−1	1	−1	1
Γ_3	2	−1	0	A_3	$H_3 2$	−2	1	−1	0	0

K	E	C	δ	E'	C'	δ'	E''	C''	δ''
K_1	1	1	1	j	j	j	j^2	j^2	j^2
K_2	1	1	−1	j	j	$-j$	j^2	j^2	$-j^2$
K_3	2	1	0	$2j$	$-j$	0	$2j^2$	$-j^2$	0

T	$\{\epsilon \mid \vec{t}\}$		$\{C_3 \mid \vec{\tau}_1+\vec{t}\}$		$\{\delta_1 \mid \vec{\tau}_2+\vec{t}\}$	
T'			$\{C_3^2 \mid \vec{\tau}_2+\vec{t}\}$		$\{\delta_2 \mid \vec{\tau}_1+\vec{t}\}$	
					$\{\delta_3 \mid \vec{t}\}$	
${}^*T_1$, ${}^*T_1'$	$3e^{2\pi i \vec{\Gamma}\cdot\vec{t}}$		0		$e^{2\pi i \vec{\Gamma}\cdot\vec{t}}$	
${}^*T_2$, ${}^*T_2'$	$3e^{2\pi i \vec{\Gamma}\cdot\vec{t}}$		0		$-e^{2\pi i \vec{\Gamma}\cdot\vec{t}}$	

M	E	δ	E'	δ'
M_1	1	1	−1	−1
M_2	1	−1	−1	1

Δ	$\{\epsilon \mid \vec{t}\}$		$\{C_3 \mid \vec{\tau}_1+\vec{t}\}$	$\{\delta_1 \mid \vec{\tau}_2+\vec{t}\}$
			$\{C_3^2 \mid \vec{\tau}_2+\vec{t}-\vec{t}_3\}$	$\{\delta_2 \mid \vec{\tau}_1+\vec{t}\}$
				$\{\delta_3 \mid \vec{t}\}$
${}^*\Delta_1$	$2\cos(2\pi\vec{k}\cdot\vec{t})$		$2\cos[2\pi\vec{k}(\vec{t}+\vec{\tau}_1)]$	0
${}^*\Delta_2$	$2\cos(2\pi\vec{k}\cdot\vec{t})$		$2\cos[2\pi\vec{k}(\vec{t}+\vec{\tau}_1)+2\pi/3]$	0
${}^*\Delta_3$	$2\cos(2\pi\vec{k}\cdot\vec{t})$		$2\cos[2\pi\vec{k}(\vec{t}+\vec{\tau}_1)+4\pi/3]$	0

Σ	$\{E \mid \vec{t}\}$	$\{C_3 \mid \vec{\tau}_1+\vec{t}\}$	$\{C_3 \mid \vec{\tau}_2+\vec{t}\}$	$\{\delta_1 \mid \vec{\tau}_2+\vec{t}\}$	$\{\delta_2 \mid \vec{\tau}_1+\vec{t}\}$	$\{\delta_3 \mid \vec{t}\}$
${}^*\Sigma$	$\sum_{i=1}^{6}\alpha_i$	0	0	0	0	0

$\alpha_i = e^{2\pi i \vec{L}_i \vec{t}}$

the Kth ion of the lth elementary cell.

Equation (3.3) can be inverted:

$$\vec{u}_\alpha(l,K)=\frac{1}{(NM_K)^{1/2}}\sum_{\vec{k}} w_\alpha(\vec{k},K)e^{2\pi i\vec{k}\cdot\vec{R}(l,K)}. \quad (3.4)$$

From equations (3.1) and (3.4), one obtains

$$\omega^2 w_\alpha(\vec{k},K)=\sum_{K'\beta} D_{\alpha\beta}(\vec{k}\,|K,K')w_\beta(\vec{k},K') . \quad (3.5)$$

In Eq. (3.5), $D(\vec{k})$ is the dynamical matrix; its elements are given in Eq. (3.6):

$$D_{\alpha\beta}(\vec{k}\,|K,K')=\frac{1}{(M_K M_{K'})^{1/2}}\sum_l \phi_{\alpha\beta}(K^l K') \times e^{-2\pi i\vec{k}\cdot\vec{R}_l}\, e^{-2\pi i\vec{k}\cdot(\vec{R}_K-\vec{R}_{K'})} . \quad (3.6)$$

Let s be the number of ions in the elementary cell. The dynamical matrix is a square matrix $3s\times 3s$. For each wave vector $\vec{k}$ the eigenfrequencies and normal modes of vibration correspond to the eigenvalues and eigenvectors of the dynamical matrix:

$$D(\vec{k})w(\vec{k})=\omega^2\vec{w}(\vec{k}) . \quad (3.7)$$

The eigenvalues are $\omega_j^2(\vec{k})$ and the eigenvectors $\vec{w}(\vec{k},j)$ where j labels the $3s$ branches of dispersion curves.

Koster[11] and Rowe[12] have shown that the symmetry group of the dynamical matrix $D(\vec{k})$ is the space group at the wave vector $\vec{k}$: $G(\vec{k})$. The vectors $w(\vec{k}\,|j)$ are transformed by any symmetry operations of $G(\vec{k})$ as irreducible representations $k^{(j)}$ of the group $G(\vec{k})$. From this result we can obtain the invariance relationships of the dynamical matrix and the projection operators necessary to calculate the normal modes of vibration.

Let $\phi=\{\alpha \mid \vec{\xi}_\alpha\}$ be an operation of the group $G(\vec{k})$ in which α is the rotation part and $\vec{\xi}_\alpha$ the nonelementary translation associated with α. Under such an operation an ion of the sublattice K will be transformed into an ion of the sublattice

$$\kappa'(K,\phi) .$$

It has been shown[13] that under the operation ϕ, the normal mode $\vec{w}(\vec{k})$ is transformed by a unitary matrix S defined as follows:

$$S^{\kappa_1\kappa_2}_{\beta,\gamma}(\vec{k},\phi)=\delta_{\kappa'(\kappa_1,\phi),\kappa_2}\alpha_{\beta,\gamma} \times e^{i\vec{k}\cdot\vec{\xi}_\alpha}e^{-i\vec{B}\cdot(\vec{R}_{\kappa_1}-\vec{\xi}_\alpha)} . \quad (3.8)$$

In Eq. (3.8), $\vec{B}$ is a reciprocal-lattice vector defined by

$$\phi\vec{k}=\vec{k}+\vec{B} \quad (3.9)$$

and $\vec{R}_{\kappa_1}$ is the lattice vector separating the elementary cell of the ion (l,κ_1) from the elementary cell of the ion deduced from (l,κ_1) by the operation ϕ:

$$\phi w_\beta(\vec{k},K_1)=\sum_{\gamma K_2} S^{\kappa_1\kappa_2}_{\beta\gamma}(\vec{k},\phi)w_\gamma(\vec{k},K_2) . \quad (3.10)$$

The set of matrices $S(\vec{k},\phi)$ is a representation of the group $G(\vec{k})$ which is the symmetry group of the dynamical matrix $D(\vec{k})$. Therefore $S(\vec{k},\phi)$ com-

TABLE V. Compatibility relations.

$\Gamma_1 \nwarrow \Delta_1$ $\Gamma_2 \swarrow \Delta_1$	$A_1 \nwarrow \Delta_2$ $A_2 \swarrow \Delta_2$
$\Gamma_3 \to \Delta_2 \oplus \Delta_3$	$A_3 \to \Delta_1 \oplus \Delta_3$
$\Gamma_1 \nwarrow T_1$ $\Gamma_2 \swarrow T_1$	$K_1 \leftarrow T_1$ $K_2 \leftarrow T_2$
$\Gamma_3 \to T_1 \oplus T_2$	$K_3 \to T_1 \oplus T_2$
$\Gamma_i \to \Sigma_i$	$M_i \to \Sigma_1$
$M_i \to T_1'$	$K_1 \to T_1'$
$M_2 \to T_2'$	$K_2 \to T_2'$
	$K_3 \to T_1' \oplus T_2'$
$K_1 \to S_1$	$H_1 \to S_2$
$K_2 \to S_1$	$H_2 \to S_2$
$K_3 \to S_2 \oplus S_3$	$H_3 \to S_1 \oplus S_3$

TABLE VI. Symmetries of the normal modes. $\alpha = 1/\sqrt{(3M+3m)}$, $\beta = 1/\sqrt{(2M+2m)}$, and $\gamma = 1/\sqrt{(6M+6m)}$.

	Hg 1			Hg 2			Hg 3			S 1			S 2			S 3		
Mode	x	y	z	x	y	z	x	y	z	x	y	z	x	y	z	x	y	z
$e^2_{\Gamma_1}=$	$\frac{1}{2}\alpha\sqrt{3M}$	$-\alpha\sqrt{(\frac{1}{2}M)}$	0	0	$\alpha\sqrt{M}$	0	$-\frac{1}{2}\alpha\sqrt{3M}$	$-\alpha\sqrt{(\frac{1}{2}M)}$	0	$\frac{1}{2}\alpha\sqrt{3m}$	$-\alpha\sqrt{(\frac{1}{2}m)}$	0	0	$\alpha\sqrt{m}$	0	$-\frac{1}{2}\alpha\sqrt{3m}$	$-\alpha\sqrt{(\frac{1}{2}m)}$	0
$e^1_{\Gamma_2}=$	0	0	$\alpha\sqrt{M}$	0	0	$\alpha\sqrt{M}$	0	0	$\alpha\sqrt{M}$	0	0	$\alpha\sqrt{m}$	0	0	$\alpha\sqrt{m}$	0	0	$\alpha\sqrt{m}$
$e^1_{\Gamma_3}=$	$\alpha\sqrt{M}$	0	0	$\alpha\sqrt{M}$	0	0	$\alpha\sqrt{M}$	0	0	$\alpha\sqrt{m}$	0	0	$\alpha\sqrt{m}$	0	0	$\alpha\sqrt{m}$	0	0
$e^{1'}_{\Gamma_3}=$	0	$\alpha\sqrt{M}$	0	0	$\alpha\sqrt{M}$	0	0	$\alpha\sqrt{M}$	0	0	$\alpha\sqrt{m}$	0	0	$\alpha\sqrt{m}$	0	0	$\alpha\sqrt{m}$	0
$e^2_{\Gamma_1}=$	$\frac{1}{2}\alpha\sqrt{3m}$	$-\alpha\sqrt{(\frac{1}{2}m)}$	0	0	$\alpha\sqrt{m}$	0	$-\frac{1}{2}\alpha\sqrt{3m}$	$-\alpha\sqrt{(\frac{1}{2}m)}$	0	$-\frac{1}{2}\alpha\sqrt{3M}$	$\alpha\sqrt{(\frac{1}{2}M)}$	0	0	$\alpha\sqrt{M}$	0	$\frac{1}{2}\alpha\sqrt{3M}$	$\alpha\sqrt{(\frac{1}{2}M)}$	0
$e^2_{\Gamma_2}=$	$-\alpha\sqrt{(\frac{1}{2}M)}$	$-\frac{1}{2}\alpha\sqrt{3M}$	0	$\alpha\sqrt{M}$	0	0	$-\alpha\sqrt{(\frac{1}{2}M)}$	$\frac{1}{2}\alpha\sqrt{3M}$	0	$-\alpha\sqrt{(\frac{1}{2}m)}$	$-\frac{1}{2}\alpha\sqrt{3m}$	0	$\alpha\sqrt{m}$	0	0	$-\alpha\sqrt{(\frac{1}{2}m)}$	$\alpha\sqrt{(\frac{3}{2}m)}$	0
$e^2_{\Gamma_3}=$	0	0	$\beta\sqrt{M}$	0	0	$-\beta\sqrt{M}$	0	0	0	0	0	$\beta\sqrt{m}$	0	0	$-\beta\sqrt{m}$	0	0	0
$e^{t2}_{\Gamma_3}=$	0	0	$\gamma\sqrt{M}$	0	0	$\gamma\sqrt{M}$	0	0	$-2\gamma\sqrt{M}$	0	0	$\gamma\sqrt{m}$	0	0	$\gamma\sqrt{m}$	0	0	$-2\gamma\sqrt{m}$
$e^3_{\Gamma_2}=$	$-\alpha\sqrt{(\frac{1}{2}m)}$	$-\frac{1}{2}\alpha\sqrt{3m}$	0	0	$\alpha\sqrt{m}$	0	$-\alpha\sqrt{(\frac{1}{2}m)}$	$\frac{1}{2}\alpha\sqrt{3m}$	0	$\alpha\sqrt{(\frac{1}{2}M)}$	$\frac{1}{2}\alpha\sqrt{3M}$	0	0	$-\alpha\sqrt{M}$	0	$\alpha\sqrt{(\frac{1}{2}M)}$	$\frac{1}{2}\alpha\sqrt{3m}$	0
$e^3_{\Gamma_3}=$	$\alpha\sqrt{m}$	0	0	$\alpha\sqrt{m}$	0	0	$\alpha\sqrt{m}$	0	0	$-\alpha\sqrt{M}$	0	0	$-\alpha\sqrt{M}$	0	0	$-\alpha\sqrt{M}$	0	0
$e^{t3}_{\Gamma_3}=$	0	$\alpha\sqrt{m}$	0	0	$\alpha\sqrt{m}$	0	0	$\alpha\sqrt{m}$	0	0	$-\alpha\sqrt{M}$	0	0	$-\alpha\sqrt{M}$	0	0	$-\alpha\sqrt{M}$	0
$e^4_{\Gamma_2}=$	0	0	$\alpha\sqrt{m}$	0	0	$\alpha\sqrt{m}$	0	0	$\alpha\sqrt{m}$	0	0	$-\alpha\sqrt{M}$	0	0	$-\alpha\sqrt{M}$	0	0	$-\alpha\sqrt{M}$
$e^4_{\Gamma_3}=$	0	0	$\beta\sqrt{m}$	0	0	$-\beta\sqrt{m}$	0	0	0	0	0	$-\beta\sqrt{M}$	0	0	$\beta\sqrt{M}$	0	0	0
$e^{t4}_{\Gamma_3}=$	0	0	$\gamma\sqrt{m}$	0	0	$\gamma\sqrt{m}$	0	0	$-2\gamma\sqrt{m}$	0	0	$-\gamma\sqrt{M}$	0	0	$-\gamma\sqrt{M}$	0	0	$2\gamma\sqrt{M}$
$e^5_{\Gamma_3}=$	$-\frac{1}{2}\alpha\sqrt{3m}$	$-\alpha\sqrt{(\frac{1}{2}m)}$	0	0	$\alpha\sqrt{m}$	0	$\frac{1}{2}\alpha\sqrt{3m}$	$-\alpha\sqrt{(\frac{1}{2}m)}$	0	$-\frac{1}{2}\alpha\sqrt{3M}$	$-\alpha\sqrt{(\frac{1}{2}M)}$	0	0	$\alpha\sqrt{M}$	0	$\frac{1}{2}\alpha\sqrt{3M}$	$-\alpha\sqrt{(\frac{1}{2}M)}$	0
$e^{t5}_{\Gamma_3}=$	$\frac{1}{2}\alpha\sqrt{3m}$	$-\alpha\sqrt{(\frac{1}{2}m)}$	0	$\alpha\sqrt{m}$	0	0	$\frac{1}{2}\alpha\sqrt{3m}$	$\alpha\sqrt{(\frac{1}{2}m)}$	0	$\frac{1}{2}\alpha\sqrt{3M}$	$-\alpha\sqrt{(\frac{1}{2}M)}$	0	$\alpha\sqrt{M}$	0	0	$\frac{1}{2}\alpha\sqrt{3M}$	$\alpha\sqrt{(\frac{1}{2}M)}$	0
$e^6_{\Gamma_3}=$	$-\frac{1}{2}\alpha\sqrt{3M}$	$-\alpha\sqrt{(\frac{1}{2}M)}$	0	0	$\alpha\sqrt{M}$	0	$\frac{1}{2}\alpha\sqrt{3M}$	$-\alpha\sqrt{(\frac{1}{2}M)}$	0	$\frac{1}{2}\alpha\sqrt{3m}$	$\alpha\sqrt{(\frac{1}{2}m)}$	0	0	$-\alpha\sqrt{m}$	0	$-\frac{1}{2}\alpha\sqrt{3m}$	$\alpha\sqrt{(\frac{1}{2}m)}$	0
$e^{t6}_{\Gamma_3}=$	$\frac{1}{2}\alpha\sqrt{3M}$	$-\alpha\sqrt{(\frac{1}{2}M)}$	0	$\alpha\sqrt{M}$	0	0	$\frac{1}{2}\alpha\sqrt{3M}$	$\alpha\sqrt{(\frac{1}{2}M)}$	0	$-\frac{1}{2}\alpha\sqrt{3m}$	$-\alpha\sqrt{(\frac{1}{2}m)}$	0	$\alpha\sqrt{m}$	0	0	$-\frac{1}{2}\alpha\sqrt{3m}$	$-\alpha\sqrt{(\frac{1}{2}m)}$	0

TABLE VII. Group representations of the normal modes.

$\Gamma = 2\Gamma_1 \oplus 4\Gamma_2 \oplus 6\Gamma_3$
$\Delta = 6\Delta_1 \oplus 6\Delta_2 \oplus 6\Delta_3$
$A = 3A_1 \oplus 3A_2 \oplus 6A_3$
$T = 8T_1 \oplus 10T_2$
$K = 2K_1 \oplus 4K_2 \oplus 6K_3$
$T' = 8T_1' \oplus 10T_2'$
$\Sigma = 18\ \Sigma_1$

mutes with $D(\vec{k})$:

$$S(\vec{k},\ \phi)D(\vec{k}) = D(\vec{k})S(\vec{k},\ \phi)\ . \tag{3.11}$$

Equation (3.11) gives all the symmetry invariants of the dynamical matrix. In order to diagonalize the dynamical matrix, we need the unitary matrix $U(\vec{k})$ which diagonalizes the matrices $S(\vec{k},\ \phi)$. This matrix can be obtained using projection operators defined as follows:

$$p^{j}_{\lambda\mu} = \sum_{\phi} k^{(j)}_{\lambda\mu}(\phi) S(\vec{k},\ \phi)\ . \tag{3.12}$$

$k^{(j)}_{\lambda\mu}$ is the $(\lambda\mu)$th element of the matrix $k^{(j)}(\phi)$ representing ϕ in the irreducible representation $k^{(j)}$ of $G(\vec{k})$. In order to fit the model parameters, we had to diagonalize the dynamical matrix in the center of the reciprocal space (Γ). The eigenvectors of displacements in the elementary cell are listed in Table VI. They are shown in Fig. 5.

We have also determined the representations of the space group corresponding to the symmetries of the dynamical matrix for every symmetry point of the reciprocal space. The results are given in Table VII.

Phenomenological Description of Model

In order to calculate the dynamical matrix $D(\vec{k})$, one must express the force matrices $\phi_{\alpha\beta}\binom{l}{K}\binom{l'}{K'}$ in terms of a potential ϕ. This potential is given using microscopic force constants which arise from two kinds of interactions: (a) The short-range valence forces are due to an overlap of the electronic orbitals. (b) The long-range Coulomb field is due to the interactions between the ionic dipole moments and the local electric field.

1. Short-Range Forces

The potential used to describe the short-range valence forces is the following:

$$\delta V_a = \frac{1}{2}\sum_{1\text{st}} \lambda[\delta r(pq)]^2$$

$$+\frac{1}{2}\sum_{2\text{nd}} \mu[\delta r(pq)]^2 + \frac{1}{2}\sum_{3\text{rd}} \nu[\delta r(pq)]^2$$

$$+\frac{1}{2}\sum_{\text{S-Hg-S}} k_\theta r_0^2[\delta\theta(ijk)]^2 + \frac{1}{2}\sum_{\text{Hg-S-Hg}} k'_\theta r_0^2[\delta\theta(ijk)]^2$$

$$+\frac{1}{2}\sum_{\text{Hg-S-Hg}} k_\phi [r_{ij}][r_{jk}][\delta\theta(ijk)]^2\ . \tag{3.13}$$

The force constants appearing in Eq. (3.13) are defined as follows:

(i) λ is a central-force constant between nearest-neighbor ions belonging to the same helix. The first sum is extended over all pairs of nearest-neighbor ions.

(ii) μ and ν are central-force constants between second- and third-neighbor ions belonging to different helices. The second and third sums are, respectively, extended over all pairs of second- and third-neighbor ions.

(iii) k_θ and $k_{\theta'}$ are the angular stiffnesses corresponding to angles S-Hg-S and Hg-S-Hg in the same helix.

(iv) k_ϕ is an angular stiffness corresponding to the angle of second- and third-neighbor S-Hg bonds with a sulfur ion at its vertex.

2. Long-Range Forces

Let $\vec{u}_j$ and $\vec{u}_i$ be the respective displacements of nearest-neighbor ions separated by a vector $\vec{r}_{ij}$ with $|\vec{r}_{ij}| = r_0$.

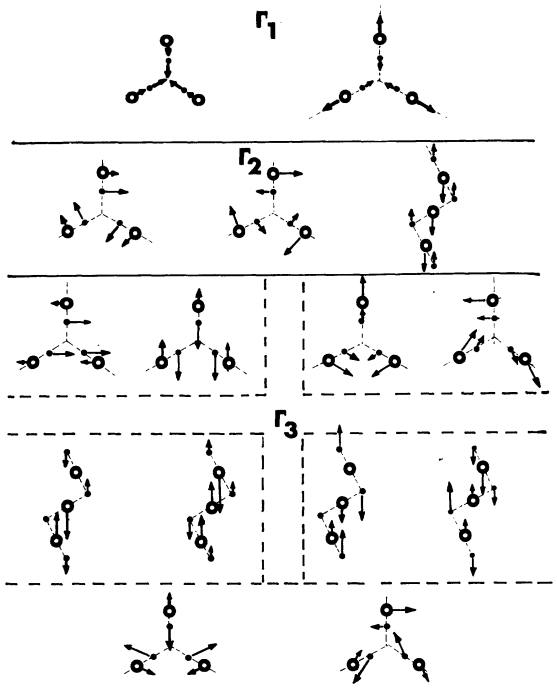

FIG. 5. Symmetry of the normal modes of vibration. The eigenvectors of the dynamical matrix are linear combinations of those modes corresponding to the same irreducible representation of the space group.

Let q_i be the ionic charge, α the polarizability of the ion i, and γ the polarization due to the deformation of the bond. The total electric dipole moment at site i is then

$$\vec{p}_i = q_i \vec{u}_i + \alpha_i \vec{E}_i + \gamma_i \sum_j \frac{\vec{r}_{ij}[\vec{r}_{ij} \cdot (\vec{u}_j - \vec{u}_i)]}{r_0^2} . \quad (3.14)$$

In the $3s$-dimensional vector space on which the dynamical matrix has its basis, Eq. (3.4) can be written

$$\vec{P} = [Q + N(\vec{k})]\vec{U} + \alpha \vec{E} . \quad (3.15)$$

In Eq. (3.15), the matrices N, α, and Q are defined by

$$\alpha_{ij} = \alpha_i \delta_{ij} , \quad (3.16)$$

$$Q_{ij} = q_i \delta_{ij} , \quad (3.17)$$

$$N(\vec{k})_{i\alpha} = \gamma_i \sum_j \frac{r_{ij}\alpha[r_{ij}(\vec{u}_j - \vec{u}_i)]}{r_0^2} . \quad (3.18)$$

$\vec{u}_i$ and $\vec{u}_j$ are expanded in terms of plane waves and therefore $N(\vec{k})$ defined by (3.18) is a function of $\vec{k}$.

The electric field E is related to the polarization vector by the relationship

$$\vec{E} = \vec{B}(\vec{k}) \cdot \vec{P} , \quad (3.19)$$

where $\vec{B}(\vec{k})$ is the Lorentz matrix which can be calculated using Ewald's method.[14]

From (3.15) and (3.19), one obtains

$$\vec{P} = [Q + N(\vec{k})]\vec{U} + \alpha B(\vec{k})\vec{P} , \quad (3.20)$$

or

$$\vec{P} = [I - \alpha B(\vec{k})]^{-1}[Q + N(\vec{k})]\vec{U} . \quad (3.21)$$

The long-range dynamical matrix is then given by

$$D(\vec{k}) = -M^{-1/2}[Q + N(\vec{k})]^{\dagger} B(\vec{k}) \times [I - \alpha B(\vec{k})][Q + N(\vec{k})]M^{-1/2} . \quad (3.22)$$

IV. RESULTS AND DISCUSSIONS

The calculation presented here is based on a simplified version of the model described in Sec. III in which the ions are supposed to be rigid ($\alpha = \gamma = 0$). The force constants were adjusted using the following experimental data:

$$\alpha_1 = \omega^2_{\Gamma_1^1} + \omega^2_{\Gamma_1^2} , \quad (4.1)$$

$$\alpha_2 = \omega^2_{\Gamma_1^1}\, \omega^2_{\Gamma_1^2} , \quad (4.2)$$

$$\alpha_3 = \omega^2_{\Gamma_2^1} + \omega^2_{\Gamma_2^2} + \omega^2_{\Gamma_2^3} , \quad (4.3)$$

$$\alpha_4 = \omega^2_{\Gamma_2^1} + \omega^2_{\Gamma_2^2} + \omega^2_{\Gamma_2^1}\, \omega^2_{\Gamma_2^3} + \omega^2_{\Gamma_2^2}\, \omega^2_{\Gamma_2^3} , \quad (4.4)$$

$$\alpha_5 = \omega^2_{\Gamma_2^1}\, \omega^2_{\Gamma_2^2}\, \omega^2_{\Gamma_2^3} , \quad (4.5)$$

$$\alpha_6 = \sum_i \omega^2_{\Gamma_3^i} . \quad (4.6)$$

In Eqs. (4.1)–(4.6), $2\pi\omega_{\Gamma_i^j}$ is the frequency of the jth normal mode with Γ_i symmetry. Those frequencies correspond to a vanishing wave vector parallel to the crystal axis. If the wave vector vanishes perpendicularly to the crystal axis, the frequencies of the Γ_2 and Γ_3 modes have different values because of the discontinuity of the macroscopic electric field. From this discontinuity we can obtain the value of the ionic effective charge q^*.

The short-range parameters λ, μ, ν, k_θ, $k_{\theta'}$, and k_ϕ have been calculated using the numerical method of Rosenbrock.[15] The best-fit values are given in Table VIII.

The calculation was done on the C.I.I. 10070 computer of the University of Rennes. The dynamical matrices were diagonalized using the Jacobi method.

The dispersion curves in directions T, Σ, M, T', k, T, Γ, Δ, and A are shown in Fig. 6. The branches are labeled by the space-group representation to which they correspond.

TABLE VIII. Model parameters.

$\lambda = 2.6204 \times 10^6$ dyn cm^{-1}
$\mu = 1.7120 \times 10^5$ dyn cm^{-1}
$\nu = 0.4679 \times 10^5$ dyn cm^{-1}
$k_\theta = -0.7873 \times 10^5$ dyn cm^{-1}
$k_{\theta'} = 2.0944 \times 10^5$ dyn cm^{-1}
$k_\phi = 0$
$q^* = 0.35e$

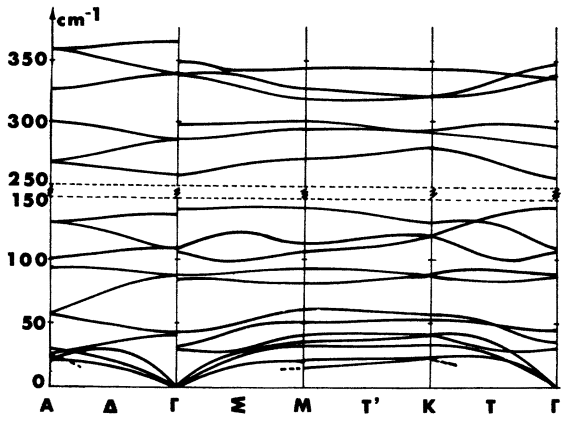

FIG. 6. Dispersion curves of the phonons in cinnabar. The dispersion curves are shown in the directions Γ-M-K-Γ-A of the first Brillouin zone.

TABLE IX. Phonon frequencies at Γ.

Symmetry	Wave vector parallel to crystal axis: Experimental frequencies[a] (cm^{-1})	Wave vector parallel to crystal axis: Calculated frequencies (cm^{-1})	Wave vector perpendicular to crystal axis: Experimental frequencies[a] (cm^{-1})	Wave vector perpendicular to crystal axis: Calculated frequencies (cm^{-1})
Γ_1	256	259	256	259
Γ_1	43	43	43	43
Γ_2	39	39	33	33
Γ_2	141	146	110	109
Γ_2	361	363	333	338
Γ_3	342	339	350	349
Γ_3	342	339	342	339
Γ_3	280	286	288	299
Γ_3	280	286	280	286
Γ_3	87	86	91	88
Γ_3	87	86	86	86
Γ_3	108	109	147	143
Γ_3	108	109	108	108
Γ_3	43	1.7	48	30
Γ_3	43	1.7	43	1.7

[a]References 2, 4, and 7–9.

The calculated eigenfrequencies at the center of the first Brillouin zone are given in Table IX and compared with the experimental values.[2,4,7–9] Except for a low-frequency T_3 mode, the agreement between our calculated results and experimental data is quite satisfactory.

We have calculated the eigenvectors corresponding to the normal modes of vibration of the crystal and we have been able to check the symmetry predicted by group-theoretical considerations.

The lower Γ_3 mode was experimentally found[2] at 43 cm^{-1}. We have not been able to calculate it with our seven parameters model. The very weak forces acting on this mode are not represented here, and we are now working on a more elaborate version of the model in order to suppress this discrepancy. The corresponding branches of dispersion have been drawn with dotted lines on Fig. 6.

Sound velocity. The slopes of the dispersion curves at the center of the first Brillouin zone indicate the sound velocities. Our calculated values are given in Table X and are compared with the available experimental values.[1] The predicted values are in close agreement with the experimental data.

TABLE X. Sound velocities in cinnabar.

	$\vec{K} \parallel c$ Theor. (m/s)	$\vec{K} \parallel c$ Expt.[a] (m/s)	$\vec{K} \perp c$ Theor. (m/s)	$\vec{K} \perp c$ Expt.[a] (m/s)
LA	2320	2450	1980	1960
TA_1	1140		1020	
TA_2	900		890	

[a]Reference 1.

The sound velocity is much slower when it propagates along a direction parallel to the x-y plane, than when it propagates parallel to the crystal axis. This is due to the very large anisotropy of the crystal.

V. CONCLUSION

The present work seems to indicate that the lattice dynamics of cinnabar can be expressed in terms of a model using a small number of microscopic parameters. We have been able to adjust seven parameters in order to fit ten optical frequencies with a vanishing wave vector parallel to the crystal axis and the eight extra frequencies with a vanishing wave vector perpendicular to the crystal axis.

An interesting feature of the phonon spectrum is that it reveals a gap. No modes are to be expected with frequencies between 150 and 250 cm^{-1}.

A mode of very low frequency could not be interpreted using the present model. A more elaborate version of a deformable-ion model will be worked out to take this discrepancy into consideration.

We must also point out the close agreement between our calculations and the measured sound velocities.

[1]J. Sapriel, Appl. Phys. Lett. 19, 533 (1971).
[2]M. A. Nusimovici and A. Meskaoui, Phys. Status Solidi (to be published).
[3]Y. Toudic and R. Aumont, J. Cryst. Growth 10, 170 (1971).
[4]R. Zalen, G. Lucovsky, W. Taylor, A. Pinczuk, and E. Burstein, Phys. Rev. B 1, 4058 (1970).
[5]M. A. Nusimovici, M. Balkanski, and J. L. Birman, Phys. Rev. B 1, 595 (1970).
[6]K. Kunc, M. A. Nusimovici, and M. Balkanski, Phys. Status Solidi 41, 491 (1970).
[7]H. Poulet and J. P. Mathieu, C. R. Acad. Sci. (Paris) 270, 708 (1970).
[8]Y. Marqueton, E. A. Decamps, B. Ayrault, and Y. Toudic, Phys. Status Solidi (to be published).
[9]J. Barcelo, M. Galtier, and A. Montaner, C. R. Acad. Sci. (Paris) 274, 1410 (1972).
[10]K. L. Aurivillius, Acta. Chem. Scand. 4, 1413 (1950).
[11]C. F. Koster, M. I. T., Solid State and Molecular Theory Groups, Technical Report No. N8, 1956 (unpublished).
[12]J. M. Rowe, Phys. Rev. 163, 547 (1967).
[13]G. Gorre, Thèse 3è cycle (Université de Rennes, France, 1972) (unpublished).
[14]P. P. Ewald, dissertation (Munich), Ann. Phys. (Leipz.) 54, 557 (1917); Ann. Phys. (Leipz.) 64, 253 (1921); Nachr. K. Ges. Wiss., Göttingen 55, 1 (1938).
[15]H. H. Rosenbrock, Comput. J. 3, 175 (1960); and G. C. Sheppey, in CERN Yellow Report No. 68-5, 1968 (unpublished).

PHYSICAL REVIEW B VOLUME 8, NUMBER 4 15 AUGUST 1973

Localization of Eigenstates in One-Dimensional Disordered Chains

Alexander Bogan, Jr.
Grumman Aerospace Corporation, Bethpage, New York 11714
(Received 7 November 1972)

A new method is presented that permits the direct calculation of a localization parameter for the wave functions in any type of one-dimensional disordered potential chain. The results agree with previous work, and extension to chains of coupled one-dimensional oscillators and electromagnetic waves in stratified media appears to be possible.

I. INTRODUCTION

The phenomenon of wave propagation in disordered materials is little understood, and theories have appeared only for the simplest systems. Recently, however, there has been a resurgence of interest in the study of these systems, stimulated mainly by the discovery of certain amorphous materials that may have electronic properties[1] of technological interest. Current literature is replete with new work on the subject, but a thorough understanding still eludes us.

Much of what we do know now is derived from studies of waves in one-dimensional systems.[2] We know, for example, that there are gaps in the density of states in amorphous as well as in crystalline materials,[3] and that eigenstates in amorphous materials are almost always localized.[4-6] We report here a method of calculating the degree of localization of the eigenstates. Whereas other techniques require either the numerical solution of a functional equation[7,8] or the computer production of sample chains,[6] our method allows us to calculate a localization parameter directly.

II. CONSTRUCTION OF TRANSFER MATRICES

We consider only potentials that may be partitioned into cells, with zero potential at the cell boundaries, as shown in Fig. 1. Schrödinger's equation is equivalent to the set of equations

$$\psi_j''(\tau) + (2m/\hbar^2)[E - V_j(\tau)]\psi_j(\tau) = 0$$

for

$$0 \le \tau \le d_j = x_{j+1} - x_j \ , \tag{1}$$

(where prime denotes differentiation with respect to the argument) along with the matching conditions

$$\psi_j(d_j) = \psi_{j+1}(0) \ , \quad \psi_j'(d_j) = \psi_{j+1}'(0) \tag{2}$$

for $j = 0, 1, \ldots, N-1$.

For a particular energy E there are always two linearly independent solutions of Eq. (1). We choose the functions $e^j(\tau)$, which satisfy the boundary conditions

$$e^j(0) = 1 \ \text{ and } \ e^{j\prime}(0) = i = (-1)^{1/2} \ , \tag{3}$$

and its complex conjugate $e_j^*(\tau)$. The wave function

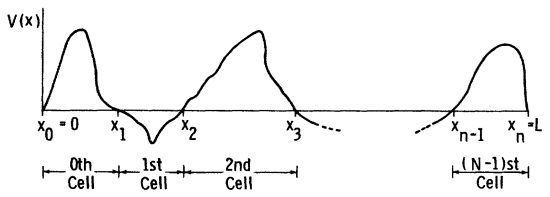

FIG. 1. Partition of the potential energy function for a one-dimensional amorphous solid into N cells.